Earth's Future

RESEARCH ARTICLE
10.1029/2023EF004149

# Can Restoring Tidal Wetlands Reduce Estuarine Nuisance Flooding of Coasts Under Future Sea-Level Rise?

**M. W. Brand[1,2,3], H. L. Diefenderfer[2,4], C. E. Cornu[5], M. A. McKeon[2], C. N. Janousek[6], A. B. Borde[2,7], T. D. Souza[8], M. E. Keogh[6,9], C. A. Brown[10], and S. D. Bridgham[9]**

[1]Louisiana State University, Baton Rouge, LA, USA, [2]Pacific Northwest National Laboratory, Coastal Sciences Division, Sequim, WA, USA, [3]University of California, Irvine, Irvine, CA, USA, [4]University of Washington, Seattle, WA, USA, [5]Institute for Applied Ecology, Corvallis, OR, USA, [6]Oregon State University, Corvallis, OR, USA, [7]Columbia Land Trust, Vancouver, WA, USA, [8]University of North Carolina, Chapel Hill, NC, USA, [9]University of Oregon, Eugene, OR, USA, [10]Pacific Ecological Systems Division, US EPA, Newport, OR, USA

**Abstract** Wetland restoration is an increasingly popular nature-based method for flood risk mitigation in coastal communities. In this study, we present a novel method using hydrodynamic modeling and harmonic analysis to quantify wetlands' ability to reduce future nuisance flooding. The method leverages a hydrodynamic model calibrated to present day data and was run for a range of future sea-level rise (SLR) and wetland restoration scenarios to quantify changes to tidal harmonic amplitudes and phases. The harmonic constituents are used to generate water surface elevations over a time period of interest (e.g., one year) and compared to critical exceedance thresholds such as levee elevations. Then, changes to nuisance flooding are calculated by counting the number of hours critical thresholds are exceeded under different SLR and wetland restoration scenarios. We applied the method to Coos Bay, Oregon, USA as a test case. We found restoration reduces the number of hours nuisance flooding occurs in downtown Coos Bay from 15 hr (present day conditions) to 0 hr (fully restored condition) under median SLR (82 cm by 2100). Restoration had spatially variable impacts on reducing peak flood elevations with minimal impacts near the estuary mouth and greatest impact 32 km inland. The effectiveness of restoration was heavily dependent on future SLR. Restoration was maximally effective in 2050 under all SLR scenarios, less effective in 2100 under median SLR, and not effective under high SLR. Modeling results suggest increased tidal prism and accommodation space are driving restoration-associated reductions in tidal amplitudes.

**Plain Language Summary** We developed a new way to estimate the flood reduction co-benefits resulting from wetland restoration in coastal bays. This is accomplished through the use of harmonic analysis trained on computational hydrodynamic models, which helps reduce computational runtimes to allow long-term analysis and run a greater number of scenarios than with physics-based modeling alone. We then applied this methodology to a study site in Coos Bay, Oregon, USA. We found that restoration can significantly reduce expected flooding in both downtown regions and along major transportation corridors in 2100 under low to moderate sea-level rise (SLR) scenarios. The expected magnitude of the flood impact reduction depended on location within the estuary and the SLR scenario. Results indicate restoration is more effective at reducing tidal flooding at inland sites, with less impacts near the coast. We also found that restoration effectiveness was driven by increased flood accommodation space, allowing floodwaters to spread.

**Key Points:**

- We developed a model which estimates reductions in nuisance flooding resulting from wetland restoration under sea-level rise (SLR)
- We apply this model to an estuary in the Pacific Northwest and find that attenuation is maximized at low and medium SLR
- We find that flood damage reduction is both spatially and temporally variable, with more benefits realized farther inland

**Supporting Information:**

Supporting Information may be found in the online version of this article.

**Correspondence to:**

M. W. Brand,
mbrand@lsu.edu

**Citation:**

Brand, M. W., Diefenderfer, H. L., Cornu, C. E., McKeon, M. A., Janousek, C. N., Borde, A. B., et al. (2025). Can restoring tidal wetlands reduce estuarine nuisance flooding of coasts under future sea-level rise? *Earth's Future*, *13*, e2023EF004149. https://doi.org/10.1029/2023EF004149

Received 21 DEC 2023
Accepted 18 DEC 2024



## 1. Introduction

Many coastal communities regularly experience predictable floods, commonly referred to as nuisance flooding (Sweet & Park, 2014). This type of flooding is characterized by the frequent inundation of low-lying areas, particularly during high tide or storm surges not directly linked to extreme weather events (Moftakhari et al., 2015). Typically, nuisance flooding does not result in catastrophic damage, but rather smaller impacts, which over time can accumulate and become comparable to extreme events (Moftakhari et al., 2017). These types of events include infrastructure damage, road closures, traffic impacts, and sewer backups (Moftakhari et al., 2018). Nuisance flooding can also decrease property values and increase insurance premiums (Moftakhari et al., 2017), with economic consequences for homeowners and businesses in affected areas (Hino et al., 2019). Nuisance flooding impacts are expected to substantially increase in coming decades resulting from sea-level rise (SLR, Fant et al., 2021; Jacobs et al., 2018; Karegar et al., 2017).

Nuisance flooding has been understudied in locations experiencing uplift, largely because those locations have to date been relatively unaffected by relative SLR. Comparison of global mean sea level (GMSL) predictions to uplift trends suggests that for most locations, there is a threshold or tipping point at which GMSL will outpace uplift (Shennan et al., 2012). Once this occurs, regions which may not have had extensive nuisance flooding issues, such as the Pacific Northwest region of the United States, may start experiencing nuisance flooding like other locations, such as the U.S. Atlantic coast (Burgos et al., 2018).

Tidal wetland restoration has been shown to reduce flooding from extreme events such as hurricanes and large coastal storms (Haddad et al., 2016; Wamsley et al., 2010). Restoration often involves reconnecting wetlands cut off from tidal influence due to levee construction (Breithaupt & Khangaonkar, 2008). Given sufficient sediment supply and inundation times, coastal wetlands are expected to keep pace with low to moderate rates of SLR, but losses and/or conversion to mudflat may occur under higher rates of SLR due to drowning and increased inundation (Alizad et al., 2022; Brand et al., 2022; Kirwan et al., 2016; Schile et al., 2014).

Wetland restoration has the potential to reduce coastal flooding via two different mechanisms: increased friction, which decreases storm surge heights (Barbier et al., 2013; Gourevitch et al., 2022; Shepard et al., 2011; Wamsley et al., 2010), and attenuation of tidal amplitude through increased tidal prism (Holleman & Stacey, 2014; Smolders et al., 2015). The reduction in coastal flooding due to increased friction is relevant to regions that experience extreme events along broad coastal plains such as hurricanes, including the Gulf Coast and Southeastern United States. These extreme events create large storm surges that locally increase water surface elevation due to decreases in barometric pressure and increases in wind setup. Wetlands reduce flooding in such cases by providing a physical barrier between an urbanized area and the coastal ocean, attenuating waves, and locally increasing friction, which reduces the energy transferred from the aquatic to the terrestrial environment (Loder et al., 2009). The broader the wetlands, the larger the reduction in storm surge height (Wamsley et al., 2010). While hurricanes do not occur in the Pacific Northwest (PNW), atmospheric rivers can induce extreme flooding events through storm surges and short-term pulses of high precipitation and streamflow in coastal watersheds (Barth et al., 2017).

The second mechanism for reducing coastal flooding by wetland restoration is through expansion of the tidal prism. Tidal prism can be increased by either management actions that allow upland migration of wetlands with SLR or by increasing intertidal wetland area. Much of the US West Coast consists of steep topography, limiting wetland migration in some regions (Thorne et al., 2018). A primary mechanism to increase tidal prism and reduce tidal amplitude is through wetland restoration via levee breaches. Modeling of San Francisco Bay, an example of an estuary with steep topography, indicates that hardened shoreline structures impact the bay's hydrodynamics by increasing tidal amplitudes up to 0.2 m, and that intertidal regions serve as energy sinks for tidal waves (Holleman & Stacey, 2014). The same model suggests that shoreline hardening can create resonance within a tidal basin, with hardening in one location resulting in greater flood risk elsewhere because higher tidal amplitudes are produced by increased tidal energy (Wang et al., 2018).

In comparison to flooding due to extreme events, nuisance flooding due to astronomic tides is relatively easy to predict because astronomic tides are a deterministic process (Ray & Foster, 2016). Tidal waves are analyzed using harmonic analysis, with tidal constituents used to decompose the tidal signal to its primary frequencies. One of the most commonly used tidal constituents in analysis is the $M_2$ constituent, which is used to describe the moon's influence on tidal water levels, and in many estuaries is the constituent with the highest amplitude (Doodson, 1928). Additionally, the $K_1$ constituent describes the moon's position in orbit relative to the Earth's equator and is especially important for describing the mixed tidal regimes along the US Pacific West coast (Flick, 2000). This study will focus on changes to both $M_2$ and $K_1$ amplitudes resulting from wetland restoration to understand potential changes to nuisance flooding.

Prediction of nuisance flooding due to astronomic tides largely depends on the choice of flood model, its calibration, and selected input values. Prediction of astronomic tides using harmonic analysis have long been studied by researchers in the context of estuarine hydrodynamics (Brand et al., 2023; Hoitink & Jay, 2016; Lu et al., 2024) and for long-term prediction of water levels (Pawlowicz et al., 2002). For example, Burgos et al. (2018) used harmonic analysis and additional statistical analysis of climate variability to predict future nuisance flooding events in Virgina. This paper differs from previous work by leveraging hydrodynamic simulations to account for the dynamic changes to tidal harmonic constituents resulting from SLR and wetland restoration and then uses those constituents to make long-term predictions of nuisance flooding.

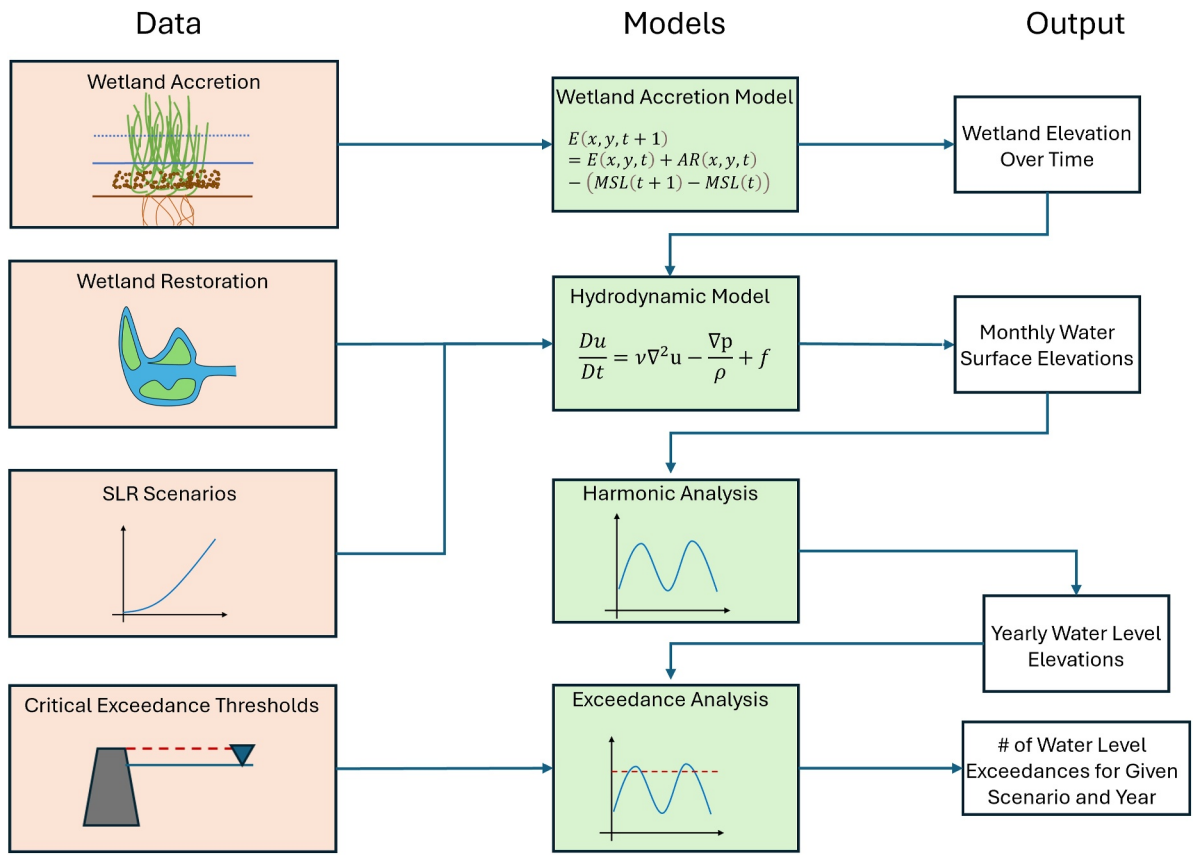


**Figure 1.** Conceptual model outline to quantify wetland restoration and sea-level rise impacts on nuisance flooding in estuarine systems.

This study addresses three research questions on coastal flood risk management.

1. Can tidal harmonic analysis trained on hydrodynamic models be used to quantify the impacts of wetland restoration and SLR on nuisance flooding?
2. What are the spatial and temporal changes to peak water levels and nuisance flooding resulting from wetland restoration, and how are those changes impacted by the spatial extent of restoration and SLR scenario?
3. What is the physical mechanism driving the impacts of wetland restoration on future nuisance flooding?

We address these questions by applying a hydrodynamic model to a climate change adaptation planning effort driven by local stakeholders in Coos Bay, Oregon, USA, which includes tidal wetland restoration as a flood management strategy.

## 2. Methods: Conceptual Framework

### 2.1. Conceptual Model Overview

The methodological approach is as follows: a hydrodynamic model is developed to capture changes to estuarine physics resulting from SLR and wetland restoration and is used to train a tidal harmonic analysis model for predicting future yearly water levels in an estuary. These water levels are then compared against critical infrastructure elevations to quantify corresponding nuisance flooding (Hydrodynamic Model and Harmonic Analysis, Figure 1). We also developed a data driven approach to calculate changes to future wetland and tidal flat elevations to capture the impacts those changes have on tidal hydrodynamics (Wetland Accretion Model, Figure 1). These changes are calculated using elevation-accretion relationships parameterized from sediment cores. Further details on each model component are described within this section.

### 2.2. Wetland Accretion Model

Wetlands respond dynamically to SLR through accretionary processes that have been shown to keep pace with low to moderate rates of SLR (Diefenderfer et al., 2021; Kirwan & Megonigal, 2013; Morris et al., 2002). To model future elevation change, we simulated the dynamic response of wetlands to SLR using an empirical model trained on measured vertical accretion rates from dated core samples of emergent marsh and tidal flats throughout the estuary (Brown et al., 2024; Eidam et al., 2023; Thorne et al., 2015, 2018; Figures S1–S3 in Supporting Information S1). This modeling approach effectively captures the inundation-accretion response that occurs in wetlands under SLR, with wetlands lower in the tidal frame experiencing higher accretion. Additionally, it constrains wetland accretion under higher SLR scenarios because wetlands are assumed to drown and convert to tidal flats (or subtidal) habitat when the depth exceeds known habitat ranges. Note that developing this model is only possible in locations with a high density of accretion data for both emergent marshes and tidal flats. In regions without significant field data to build a semi-empirical model, one could use marsh equilibrium models such as the Hydro-MEM (Alizad et al., 2016, 2018) or WARMER (Thorne et al., 2018).

Elevation-accretion relationships were created separately for emergent marshes and tidal flats. Locations and measured accretion rates for all core samples are shown in Figure S1 in Supporting Information S1. Emergent marshes were defined as intertidal areas with initial elevations between 1.6 and 2.6 m above North American Vertical Datum of 1988 (NAVD88) based on core sample elevations (Figure S2 in Supporting Information S1, $n = 14$) collected throughout the estuary. This information was used to construct an empirical relationship between marsh elevation and accretion (Equation 1).

$$\mathrm{AR}(x,y,t) = -3.382 * E(x,y,t) + 10.25 \tag{1}$$

where AR($x$, $y$, $t$) and $E(x, y, t)$ are accretion rate at point $x$, $y$ and time step $t$ (in mm/yr), and elevation point at $x$, $y$ and time step $t$ (in m NAVD88), respectively.

No relationship was found between elevation and accretion in tide flats (Figure S3 in Supporting Information S1), so we modeled them using a yearly averaged accretion rate measured across all samples in the estuary ($n = 11$, Equation 2). Tidal flat elevations were modeled between −2.15 and 1.6 m NAVD88.

$$\mathrm{AR}(x,y,t) = 0.00542 \tag{2}$$

We calculated future yearly marsh and tidal flat elevations by propagating surface elevations using the elevation/accretion relationships in Equations 1 and 2, less SLR at that timestep (Equation 3).

$$E(x,y,t+1) = E(x,y,t) + \mathrm{AR}(x,y,t) - (\mathrm{MSL}(t+1) - \mathrm{MSL}(t)) \tag{3}$$

where $E(x, y, t)$ is marsh or tidal flat elevation at point $x$, $y$ and time step $t$, AR($x$, $y$, $t$) is the accretion at point $x$, $y$ and time step $t$ from Equations 1 or 2, MSL($t+1$) and MSL($t$) are mean sea level at time $t+1$ and $t$, respectively.

The transition from emergent marsh to tidal flats (and vice versa) was assumed to occur over the year timestep and was modeled by switching between Equations 1 and 2 for accretion depending on the marsh planform elevation relative to mean sea levels at that timestep. Areas considered subtidal (below tidal flat elevations) were assumed to not accrete. Note that this model is decoupled from the hydrodynamic model and serves to update marsh and tidal flat elevations in the hydrodynamic model for the years 2050 and 2100.

### 2.3. Model Coupling and Outputs

Tidal water levels must first be predicted using a hydrodynamic model, calibrated to measured water levels using existing or collected data sets. Data inputs include topobathymetry, hydrodynamic roughness, and astronomic tidal boundary conditions for the years of interest. Then, a set of wetland restoration and SLR scenarios are developed in collaboration with stakeholders (Figure 1). Key model outputs are timeseries of water levels in locations identified during the stakeholder engagement process, for example: urban cores, agricultural land, levees, airports, and other critical infrastructure.

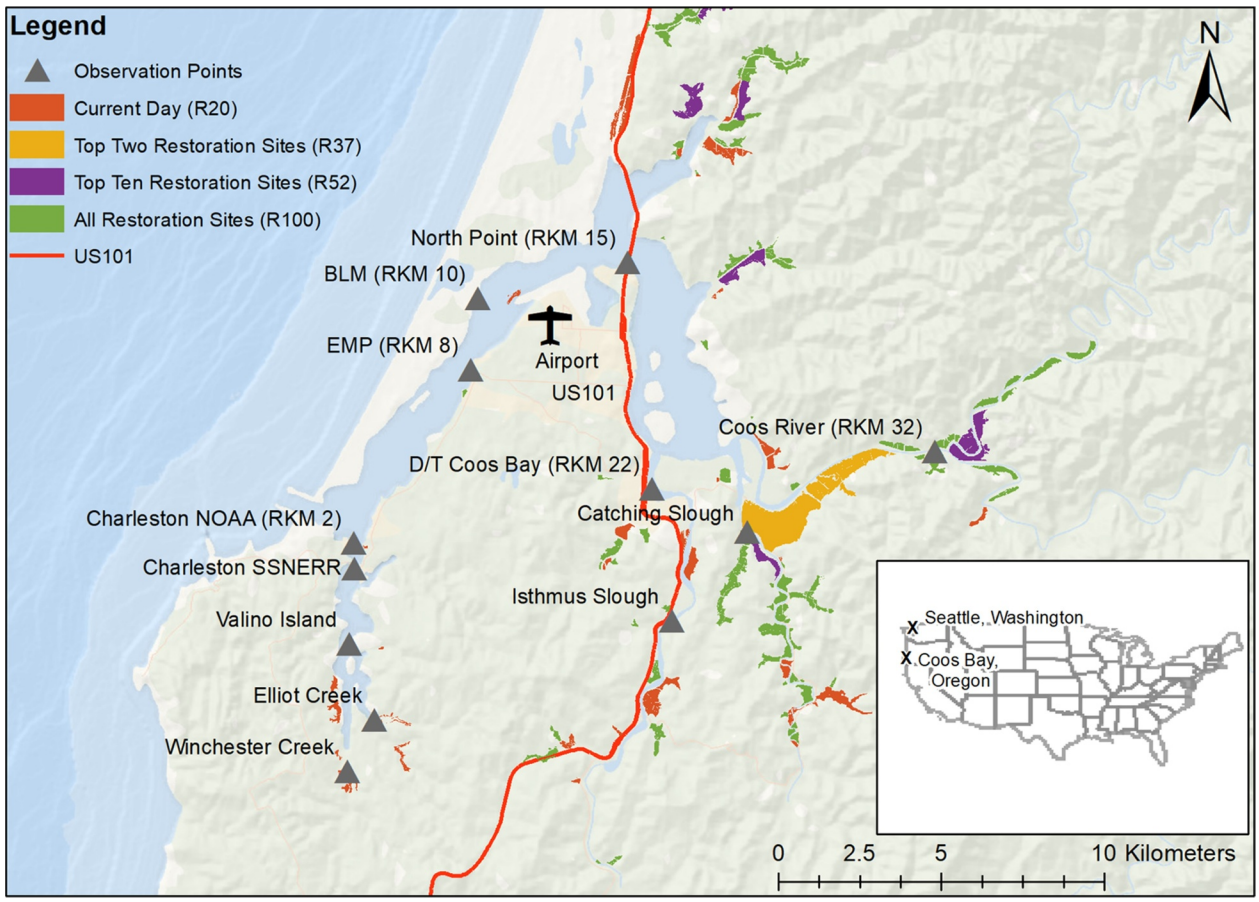


**Figure 2.** Map of Coos Bay, Oregon, with water level data observation points (gray dots), US 101 (red line), and four of the five restoration scenarios modeled in this study. An additional "no restoration" (R0) scenario incorporated all levees within the current day (2023, orange polygons) scenarios plus levees from previously restored wetlands.

Hydrodynamic model outputs are used to estimate tidal constituents and calculate annual water levels for each location of interest using harmonic analysis (i.e., *t_tide* from Pawlowicz et al., 2002) for present day and future water levels resulting from both wetland restoration and SLR (Figure 1). The benefit of harmonic analysis is that tidal predictions can be calculated nearly instantaneously (in a matter of seconds on a single-core desktop using the *t_predic* function from Pawlowicz et al., 2002) compared to full hydrodynamic simulations (which often take hours to days on high performance computers).

The number of exceedances are then calculated using water levels from the harmonic analysis (Figure 1). Examples of exceedance thresholds include the number of times a levee protecting a downtown core is overtopped, or the elevation of critical infrastructure such as airports, water treatment plants, or highways. This information is then used to identify the wetland restoration scenarios that are most effective at mitigating future nuisance flooding for a given level of SLR.

## 3. Model Application

### 3.1. Site Description

We applied the above methodology to Coos Bay, Oregon (Figure 2), a drowned river mouth estuary (Lee & Brown, 2009) located on the southern coast of Oregon in the Pacific Northwest region of the United States approximately 380 km south of Seattle, Washington. It is the state's second largest estuary at 54 $km^2$ (Rumrill, 2006), and is surrounded by multiple communities, including the cities of Coos Bay and North Bend and the unincorporated community of Charleston, which have a combined population of 64,929 (United States Census

**Table 1**
*Projected Change in Mean Sea Level in Coos Bay by 2050 and 2100 for Modeled Sea-Level Rise Scenarios (From DP16 Scenario of Kopp et al., 2017)*

| | Year | |
|---|---|---|
| Scenario | 2050 | 2100 |
| Low (RCP2.6, bottom 5%ile) | −1 cm | 7 cm |
| Median (RCP4.5) | 18 cm | 82 cm |
| High (RCP8.5, top 95%ile) | 43 cm | 251 cm |

Bureau, 2022). The estuary is fed by multiple rivers, the largest being the Coos River, which has a highly variable seasonal discharge (~500 $m^3$/s at peak stage with summer baseflow of 1 $m^3$/s, Conroy et al., 2020) and greater diurnal tidal range of 2.32 m (NOAA, 2023). The estuary contains 2,427 ha of intertidal habitat (Borde et al., 2003), which supports a variety of estuarine wetland types, including oyster beds, seagrass meadows, tide flats, emergent marsh, and tidal swamps. Historically, the estuary has been extensively modified, including the ongoing dredging of a navigational channel for a commercial port, which has increased mean tidal range by 33% through a reduction in main channel friction (Eidam et al., 2020). Coos Bay's vertical uplift is estimated at 1.1 mm $yr^{-1}$, while SLR rates measured at the estuary's NOAA (Charleston) tide gauge over the last 5 decades are 1.0 mm $yr^{-1}$, giving an estimated current relative SLR of −0.1 mm $yr^{-1}$ (NOAA, 2023; Sweet et al., 2017).

Overall, the estuary has experienced an estimated 73%–90% loss of tidal wetland area since pre-Euro-American settlement because of filling for urban development and diking and draining for agricultural uses (Brophy, 2019). The converted wetlands and remaining estuarine habitats still support a variety of commercial and recreational fisheries as well as a robust ecotourism industry. Most potential restoration sites in the estuary are former wetlands converted to agricultural land. These former wetlands (1,700 ha) would regularly flood from high tides if they were not leveed and drained.

Most rainy seasons, downtown merchants in Coos Bay must protect their properties (built on filled former tidal wetlands) from storm-driven tidal flooding. Occasionally, they face more significant flooding, for instance, during flooding caused by a series of storms in 1996. Many of these vulnerable businesses are situated in low-lying locations on US Highway 101 (US 101), a major regional transportation artery running along the Oregon coast and the principal roadway through the study area.

### 3.2. Community-Driven Research

We engaged community leaders through local partnerships and co-developed a flood model of Coos Bay to meet community concerns and needs. This engagement was primarily accomplished through monthly meetings of the Partnership for Coastal Watersheds, a Coos Bay area stakeholder group consisting of scientists, government representatives, non-governmental organizations, and local business leaders. Potential restoration and critical infrastructure areas were identified with the Coos Estuary Restoration Opportunity Inventory, developed by members of the partnership. Critical infrastructure identified includes the Southwest Oregon Regional Airport, US 101, and downtown Coos Bay (Figure 2). The airport is built on a peninsula extending into the bay itself, and along with downtown Coos Bay (D/T Coos Bay, Figure 2), is protected by a network of levees. The highway is currently subject to closures as a result of flooding and is considered by local stakeholders to be especially vulnerable to future SLR.

### 3.3. Sea-Level Rise, Nuisance Flooding, and Restoration Scenarios

We developed hydrodynamic modeling boundary conditions using SLR scenarios based on three scenarios representing high, low, and median SLR estimates for Coos Bay, derived from Kopp et al. (2017) using the DP16 estimates for the years 2050 and 2100 (Table 1). These scenarios are compared to the most recent AR6 estimates (Fox-Kemper et al., 2021; Gerner et al., 2021; Kopp, Garner, et al., 2023) below. The low SLR scenario bound was the bottom of the 95% confidence interval of Representative Concentration Pathway 2.6, which is the "low emissions scenario" defined by the Intergovernmental Panel on Climate Change and used in climate and SLR models (IPCC, 2014). This scenario results in 7 cm of SLR by 2100 compared to 11 cm of SLR for the SSP1-2.6 "medium confidence" scenario in AR6 (Garner et al., 2021). The high bound used in this study was the top 95% confidence interval of the RCP8.5 scenario used in Kopp et al. (2017), which represents "very high" fossil fuel usage and is comparable to the 95th percentile "low-confidence" (which accounts for uncertain ice-sheet processes) high emissions SSP5-8.5 in the IPCC's 6th assessment report (Fox-Kemper et al., 2021), which estimates 225 cm of SLR for the Charleston gauge (compared to 251 cm for this study). The median SLR scenario used in this study was the 50th percentile estimate of SLR from RCP4.5 in (Kopp et al., 2017), which is defined as an "intermediate scenario." This scenario is within 1 cm of the "intermediate" scenario at the Charleston gauge from

**Table 2**
*Marsh Restoration Scenarios Used in This Study for Coos Bay*

| Scenario | Description | % Restored |
|---|---|---|
| R0 | Pre-Restoration conditions (circa 1960) | 0% |
| R20 | Present-day conditions | 20% |
| R37 | Largest two sites restored | 37% |
| R52 | Top 10 sites restored | 52% |
| R100 | All feasible sites restored | 100% |

the Sweet et al. (2022) NOAA SLR scenarios report for the United States, and is 39 cm higher compared to the SSP2-4.5 "medium confidence" scenario in the IPCC's 6th assessment report (Fox-Kemper et al., 2021; Garner et al., 2021). There are no simulations which currently evaluate a "low confidence" scenario for SSP2-4.5 (Kopp, Oppenheimer, et al., 2023).

Nuisance flooding was defined following Moftakhari et al. (2017) as regularly occurring tidally related flooding in which flood depth exceeds 3 cm. We calculated transportation infrastructure flooding (US highway 101) by quantifying the number of minutes a hydrodynamic element along the highway exceeded 0.03 m in depth for each simulation. Similarly, we calculated flooding of downtown Coos Bay by counting the time that water levels exceeded the levee elevations protecting downtown.

We examined five marsh restoration scenarios (Table 2), with restoration simulated as full levee removal for a site within the hydrodynamic model. The pre-restoration scenario included levees present before the last several decades of ecosystem restoration by levee breach and removal, when leveed land was at its peak circa 1960. This scenario (R0, Table 2) was a baseline, with 0% tidal area restored. The four additional scenarios were based on maps of former tidal wetlands converted to agricultural uses that defined the maximum extent of feasible restoration in the estuary. This excluded urban regions in former tidal wetlands because they often include fill, which makes restoration much more expensive compared to agricultural regions, which primarily involves levee breaching or removal.

The present day scenario simulated current conditions, with 20% of the overall former tidal wetland land surface within Coos Bay restored, excluding urban areas (R20, Table 2). The R37 restoration expansion scenario modeled a potential restoration of 37% above the R0 condition, incorporating all restoration to date (R20) plus the largest two potential restoration sites within Coos Bay, both located along the Coos River, upriver of the confluence with Catching Slough (yellow areas, Figure 2). The R52 restoration expansion scenario included all sites in the R37 scenario plus the top eight additional potential wetland restoration sites by land area, totaling 52% of overall potential restoration areas (in purple, Figure 2). Finally, the R100 wetland expansion scenario considered wetland restoration at all feasible sites within the modeled maximum tidal boundary where former tidal wetlands were historically converted to agricultural uses. Each scenario only considered areas restorable to intertidal marsh or swamp habitats, not areas where elevation is too low, including open water, eelgrass, and mudflat regions.

### 3.4. Hydrodynamic Model Description and Calibration

We developed the hydrodynamic model using Delft3D-FM (version 2021.03, Kernkamp et al., 2011; Lesser et al., 2004) with 372,142 elements and 191,284 nodes, and a variable horizontal resolution that ranged from 4 km offshore to 5 m at the mouth of the estuary and 2 m in upriver reaches and wetlands. Model runtimes for a 1-month simulation (including 7-day of model spin up) took 3.5–4 hr on a 64-core high-performance computing system. We interpolated the model mesh to a mosaic bare-earth topobathymetric surface from data sources provided by Conroy et al. (2020) and a LiDAR (Light Detection and Ranging) survey by the US Army Corps of Engineers in 2014 (OCM Partners, 2023). The model contained 324 levees from the Oregon Levee Data set (O'Brien, 2017). Levee elevations were enforced on the mesh using the "fixed weir" tool in Delft3D-FM, which intersects levee elevations in the model mesh. This method allows water to flow over the enforced elevation of the grid cell edge, with no flow under that elevation.

We interpolated floodplain and wetland model roughness to the hydrodynamic mesh using the 10-m resolution National Land Cover Database (NLCD) data set (U.S. Geological Survey, 2019) and HEC-RAS manual to assign Manning's $n$ values from land-use classes (Brunner, 2024; Table S1 in Supporting Information S1). The calibrated main channel and offshore roughness were 0.027 and 0.015, respectively (Figure S4 in Supporting Information S1). We manually modified the Manning's $n$ value to follow the main channel in locations where the model mesh resolution was finer than the underlying NLCD data set, such as Winchester Creek. Typical wetland roughness values were 0.027–0.046 for herbaceous to scrub/shrub wetlands.

The hydrodynamic model calibration time period was forced following Conroy et al. (2020), with tidal water levels generated offshore using the TPXO tidal data set (Egbert & Erofeeva, 2002) and non-tidal residuals

calculated using the difference between measured and predicted tidal water levels at the NOAA tide gauge in Charleston, Oregon. Fluvial boundary conditions for wintertime model calibration (total of 14) were provided and described by Conroy et al. (2020). The hydrodynamic model was calibrated to 10 stations throughout the estuary with observed water depth and surface elevation data (gray dots, Figure 2) using Root Mean Square Error (RMSE, Equation 4) as the calibration variable.

$$\mathrm{RMSE} = \sqrt{\frac{1}{N}\sum_{t=1}^{N}(x_t - \hat{x}_t)^2} \tag{4}$$

Where $x_t$ is the hydrodynamic model water level prediction, $\hat{x}_t$ is the harmonic or measured model water level prediction, $t$ is the timestep, and $N$ is the total number of high-water level samples. High water levels were found using MATLAB's *findpeaks* function using a "minimum peak distance" of 100 min.

The model calibration process included modifying mesh resolution and Manning's $n$ values. Overall water level RMSE's averaged 10 cm and high water level RMSE's averaged 7.5 cm. Overall, the hydrodynamic model performed nearly equivalently to the Conroy et al. (2020) model for all calibration stations using the $R^2$ calibration metric (Table S2 in Supporting Information S1). Additionally, we tested the hydrodynamic model's performance using the RMSE metric for water level and high-water level measurements. The overall water level RMSE averaged 9.9 cm and ranged from 5.1 to 15.7 cm throughout the model domain, with the lowest RMSE nearest the estuary mouth (NOAA, RKM 2), and generally increasing up-estuary (Coos River, RKM 32, Table S2 in Supporting Information S1). The average high-water RMSE was 7.5 cm, ranging from 4.5 to 11 cm, with a similar increase in RMSE moving up-estuary compared to locations closer to the coastline.

In addition to calibration to point sources of data, the model was further validated against an observed spring tide data set collected by the authors on 4 December 2021. We took time-stamped photographs at three locations during the peak high-water event in the spring tide period and compared these field observations to the areal extent predicted by the model. The locations were along US 101 south of downtown Coos Bay and just north of downtown Coos Bay at places known to previously flood. Overall, the extent of flooding seen in the field was matched by model output; photographs and observations of flooding extent compared to model outputs are shown in Figures S5–S8 in Supporting Information S1.

### 3.5. Future Hydrodynamic Model Boundary Forcing & Validation

Future model forcing for the oceanic boundary condition simulated a full month (December) of tidal water levels for the years 2050 and 2100, using the December 2021 water levels as a boundary condition as the baseline water level (Figure S9 in Supporting Information S1), and adding the corresponding SLR scenario to the water levels (Table 1). This slightly deviates from the methodology outlined in Section 2.3 to ensure that we were comparing the same water levels for calculating reductions in nuisance flooding resulting from wetland restoration. Water levels were driven by tidal constituents from the TPXO tidal model (Egbert & Erofeeva, 2002) and converted to water levels using the *t_predic* function from Pawlowicz et al., 2002, with a 7-day model spin up period simulated prior to December. Offshore water levels were converted from mean sea-level to NAVD88 using VDatum (1.18 m offset). We did not include fluvial boundary inputs or wind in the future runs.

## 4. Results

The results section is organized as follows: first, we compare the accuracy of the harmonic model against the hydrodynamic model (Section 4.1). Then, we present the results of the marsh and tidal flat accretion model (Section 4.2). These elevations were used to update the topobathymetry in the hydrodynamic model. Hydrodynamic model outputs were used as inputs to the harmonic analysis to quantify the impacts of wetland restoration on projected nuisance flooding in Coos Bay in 2050 and 2100 (Section 4.3). We further present results on the changes to the spatial distribution and impacts on transportation infrastructure due to wetland restoration (Section 4.4). Finally, we use harmonic analysis and changes to tidal prism to present results on mechanistic contributors to nuisance flood reduction (Section 4.5).

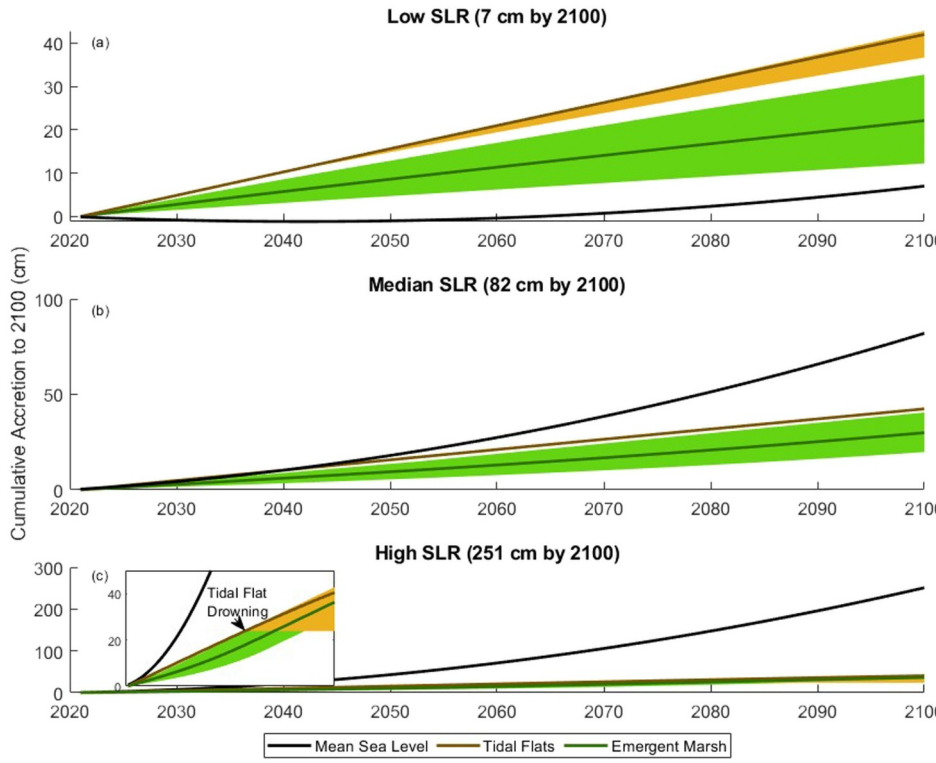


**Figure 3.** Projected tidal flat and emergent marsh elevation and mean sea level in Coos Bay from 2020 to 2100 under three sea-level rise scenarios modeled in this study (low = a, median = b, and high = c) based on the empirically derived models of vertical accretion. Dark green and brown lines represent the mean emergent marsh and mean tidal flat elevations, respectively, and the green and orange color bands represent the 95% confidence intervals for marsh and tide flat elevation, respectively. Note that the "High SLR" (c) scenario has a zoomed inset at the scale of tidal marsh and mudflat accretion demonstrating tidal flat and marsh drowning.

### 4.1. Harmonic Model Performance

The RMSE between the harmonic model and hydrodynamic model was smallest near the estuary mouth (average of 3.8 cm at RKM 2) and increased up-estuary, with an average of 5.8 cm at RKM 32 (Figure S13 in Supporting Information S1). This effect is due to the more complex tidal hydrodynamics resulting from tidal wave deformation farther up-estuary compared to near the estuary mouth. There was not a discernible difference in RMSE values between the hydrodynamic and harmonic models for different SLR scenarios, and no obvious trends in RMSE between restoration (R0 through R100, Figure S13 in Supporting Information S1).

### 4.2. Marsh and Tidal Flat Accretion Under Sea-Level Rise

The wetland accretion simulations indicated that marsh and tidal flat elevation increases outpace low SLR rates (Figure 3a) but not under median and higher SLR (Figures 3b and 3c). Overall, average tidal flat accretion outpaced emergent marsh accretion for all SLR scenarios. Some tidal flat accretion stops around the year 2037 in the high SLR scenario (inset of Figure 3c) because lower tidal flats are drowned and converted to subtidal depths, where the model assumes a fixed bed. These results for each SLR scenario were sampled in the years 2050 and 2100 and used to update the topobathymetry in the respective hydrodynamic model.

### 4.3. Effects of Wetland Restoration on Projected Urban Nuisance Flooding

Expanded wetland restoration (R37, R52, and R100) reduced projected nuisance flooding in downtown Coos Bay by dampening the tidal signal and reducing high water surface elevations under the median SLR scenario (Figure 4). The low SLR scenario did not result in any nuisance flooding in the estuary (Figure 4c), while the high SLR scenario resulted in very significant flooding (over 4,800 hr a year, or 240 days; Figure 4e).

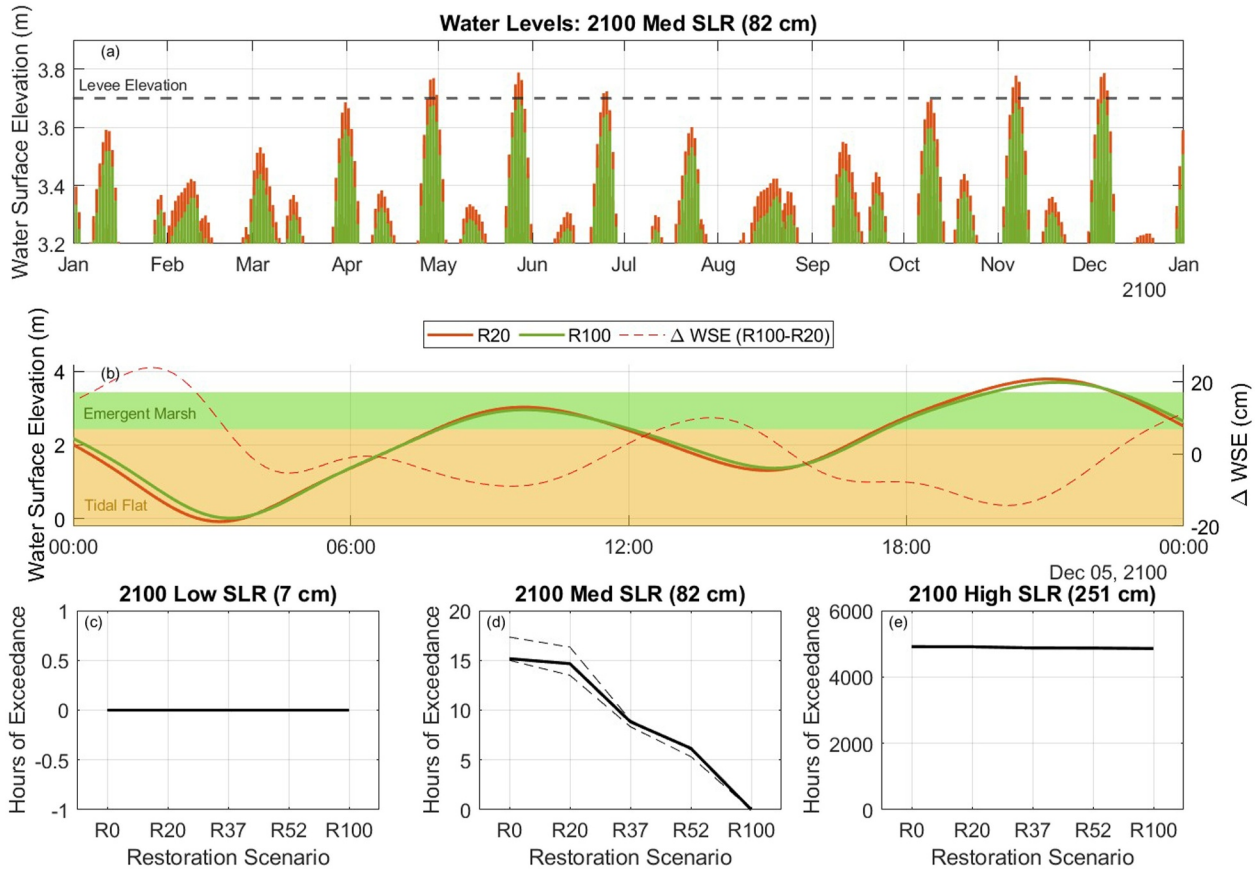


**Figure 4.** Projected water surface elevations in Coos Bay (downtown) using harmonic model for 2100 (a) under the present-day restoration scenario (orange line, R20) and full potential restoration scenarios (green line, R100). The selected critical exceedance threshold ("Levee Elevation") is shown as a black dashed line on the full time series (a). We also highlight changes to the water surface elevations in the context of the emergent marsh and tidal flat elevations for 5 December 2100 (b). Note that mudflat and emergent marsh elevations are shown in yellow and green shaded regions, respectively, with the difference in water surface elevations (R100-R20, reductions are negative values) shown as the dashed red line. Increasing extent of restoration decreases the number of hours of levee exceedance from 15 hr for 2100 (R0) to 0 hr (R100), bottom row, panel (d) under the median sea-level rise (SLR) scenario, and from 4,912 (R0) to 4,856 hr (R100) under the high SLR scenario (e). 95% confidence bounds resulting from uncertainty in the harmonic analysis are shown as dashed black lines in panel (d). There is no levee exceedance under low SLR (panel c).

Present day wetland restoration efforts (from R0 to R20) have resulted in a decrease of expected flooding from levee overtopping in downtown Coos Bay from 15.2 to 14.6 hr in 2100 under the median SLR scenario (Figure 4d). Further restoration efforts will considerably reduce projected nuisance flooding with 37% restoration (R37), 52% restoration (R52), and 100% restoration (R100) resulting in 8, 3, 6.1, and 0 hr, respectively, of levee overtopping (Figure 4d).

Wetland restoration had spatially variable effects on the highest (peak) water surface elevations modeled in the estuary (pWSE). The reduction in pWSE due to restoration was smallest near the estuary mouth under all SLR scenarios (Figure 5). The greatest modeled reductions in pWSE (~10 cm) were under the low and median SLR scenarios, which occurred east of downtown Coos Bay for the low SLR scenario, or near North Point and Catching Slough under the median SLR scenario (Figure 5a).

The areas with the greatest increase in pWSEs in the low SLR scenario include restored wetlands, such as those just east of the Catching Slough station. This is a direct effect of the levee removal implemented to bring about wetland restoration. However, under the median 2100 SLR scenario, this area experienced a 2–4 cm reduction in pWSE with full wetland restoration, with the adjacent eastern region seeing a reduction of more than 10 cm (Figure 5b). This occurs because these areas, which are currently leveed, were overtopped in the median SLR scenario regardless of whether wetland restoration occurs. There was no reduction in pWSE due to wetland restoration under the highest SLR scenario (Figure 5c).

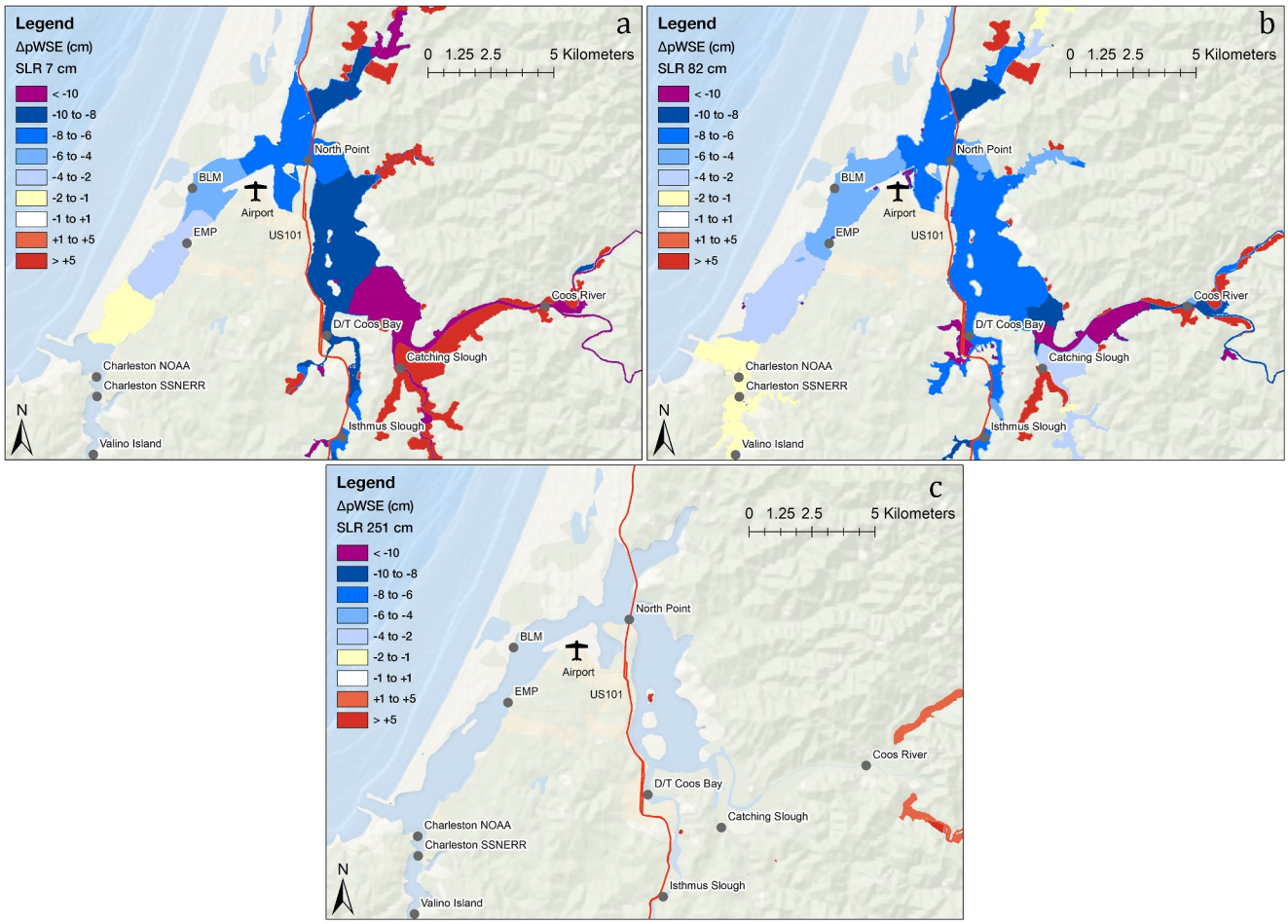


**Figure 5.** Spatial variability of change in peak water surface elevation (pWSE) resulting from full wetland restoration (R100-R20) during the simulated spring tide event under the low 7 cm (a), median 82 cm (b), and high 251 cm (c) sea-level rise scenarios in December 2100. Note that negative values indicate a reduction in pWSE, with positive values indicating an increase in pWSE.

### 4.4. Effects of Wetland Restoration on Urban Flood Extent and Transportation Infrastructure

Reductions in pWSE from wetland restoration also reduced the areal extent of nuisance flooding due to SLR. Under the median estimated SLR with no restoration (R0), a significant portion of downtown Coos Bay would regularly flood during spring tides by 2100 (Figure 6a). In these events, both lanes of US 101 would flood to depths greater than 30 cm, with >50 cm of water on the northbound lanes over a 700-m span. Under the full restoration (R100) scenario, the extent of this flooding would be reduced; the southbound lane of US 101 would no longer be blocked (Figure 6b).

Sea-level rise and restoration also impacted the duration of flooding of transportation infrastructure. The number of hours that US 101 was inundated by more than 3 cm of water for the simulated spring tide is shown in Table 3 for the years 2050 and 2100. For the year 2050, there is no projected tidal flooding of US 101 under the low (−1 cm) SLR scenario, similar to present-day conditions. Under the median (18 cm) of SLR by 2050, US 101 is predicted to flood for 1 hr in December for both the current condition (R20) and no-restoration (R0) scenarios, but this would be reduced to 0 hr for the R37, R52, and R100 scenarios. Under the high (43 cm) SLR scenario, US 101 would be flooded for 19 hr under R0 and R20 scenarios. Restoration progressively reduces the time that US 101 is anticipated to flood, with R37 resulting in 15 hr of flooding, and R100 resulting in only 12 hr of flooding.

Regular flooding of US 101 is projected to become common in 2100 under the median and high SLR scenarios in Coos Bay. Under the low (7 cm) SLR scenario there would be no flooding, but median (82 cm) SLR would result in nearly 100 hr of flooding under R20. Full wetland restoration would reduce the number of hours flooded from

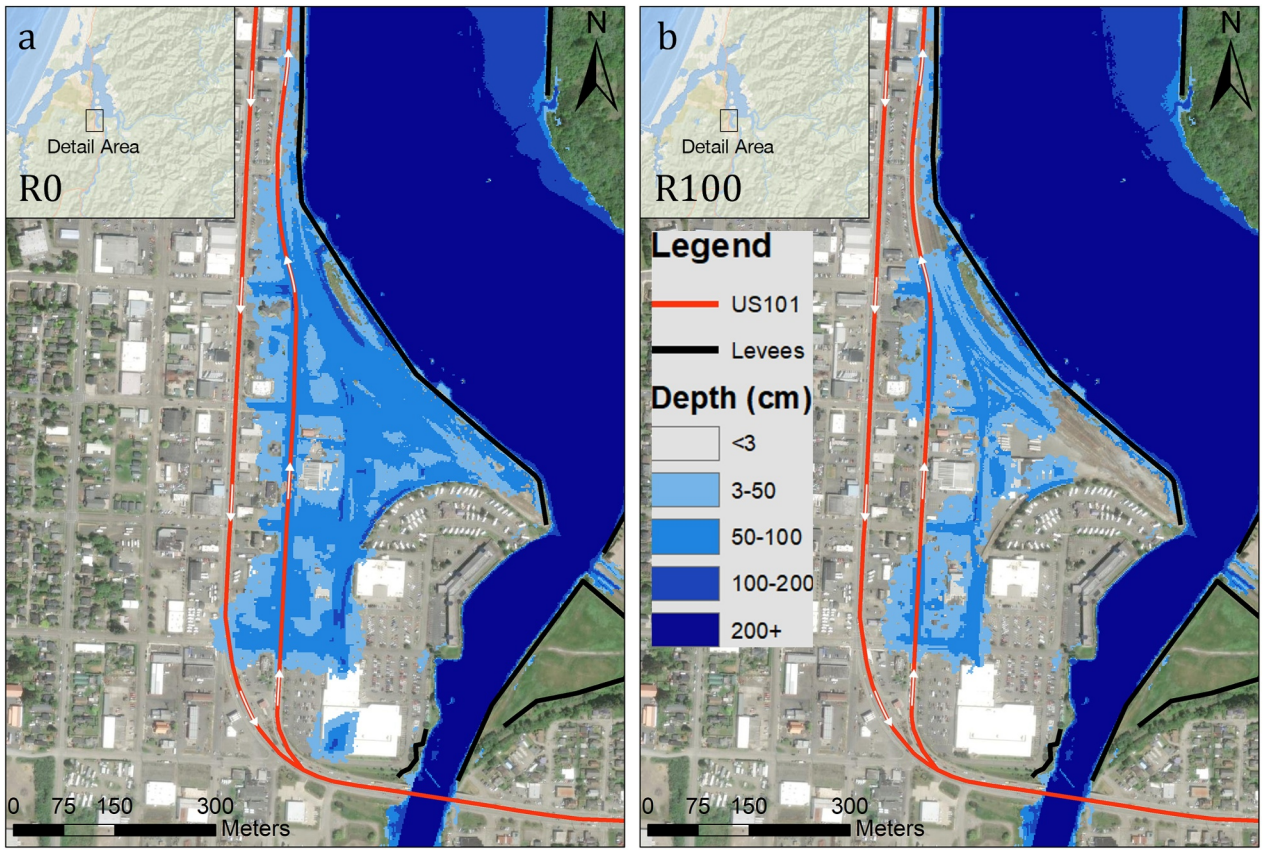


**Figure 6.** Modeled areal extent of flooding (depth in cm) along US Highway 101 (red lines) and in downtown Coos Bay under the median (82 cm) sea-level rise scenario for December 2100 for (a) the no-restoration (R0) scenario and (b) the 100% (R100) restoration scenario. White arrows show the direction of traffic along US 101.

99 to 85, a 14% reduction. The highest SLR scenario (251 cm) would result in near-continuous flooding of US 101 for almost the entire month (there are 744 hr in a month).

### 4.5. Wetland Restoration and Sea-Level Rise Impacts on Tidal Harmonics and Hydrodynamics

Model results indicated $M_2$ tidal constituent has the largest amplitude within Coos Bay compared to the other 29 calculated constituents (amplitude of 79–88 cm compared to $K_1$ amplitude of ~42–45 cm). $M_2$ was amplified as it traveled farther inland for all SLR scenarios and dampened as the estuary becomes constrained at river kilometer 34 (RKM 34, Figure 7). Wetland restoration significantly dampened the $M_2$ constituent under all SLR scenarios at all stations except near the estuary mouth (RKM 2, NOAA), where there was minimal effect. The largest dampening occurred at the Coos River station (RKM 32); in 2100, for example, the $M_2$ amplitude was reduced by 13 cm under median SLR for full restoration (R100) (Figure 7e). Wetland restoration did not significantly change the $M_2$ phase under low SLR scenarios, except farther up the estuary near RKM 32, where the phase was increased by ~10° (Figure S12 in Supporting Information S1). Under median and high SLR scenarios the $M_2$ phase increased from both SLR and wetland restoration in inland regions (RKM 15 and above), with the effect increasing farther inland (Figure S12 in Supporting Information S1).

Modeled reductions in pWSEs due to increased restoration were associated with an increase in the overall tidal prism (Figure 8). The relationship between the increase in tidal prism and reduction in pWSE with increasing restoration intensity is projected to be linear for the low SLR scenario until

**Table 3**
*Number of Hours Any Lane of US 101 Is Projected to Flood as a Function of Sea-Level Rise and Wetland Restoration Scenario During December 2050 and 2100*

| | | Restoration scenario | | | | |
|---|---|---|---|---|---|---|
| | | R0 | R20 | R37 | R52 | R100 |
| YR 2050 | −1 cm | 0 | 0 | 0 | 0 | 0 |
| | 18 cm | 1 | 1 | 0 | 0 | 0 |
| | 43 cm | 19 | 19 | 15 | 14 | 12 |
| YR 2100 | 7 cm | 0 | 0 | 0 | 0 | 0 |
| | 82 cm | 100 | 99 | 97 | 93 | 85 |
| | 251 cm | 734 | 734 | 735 | 735 | 732 |

*Note.* There are 744 hr in a month.

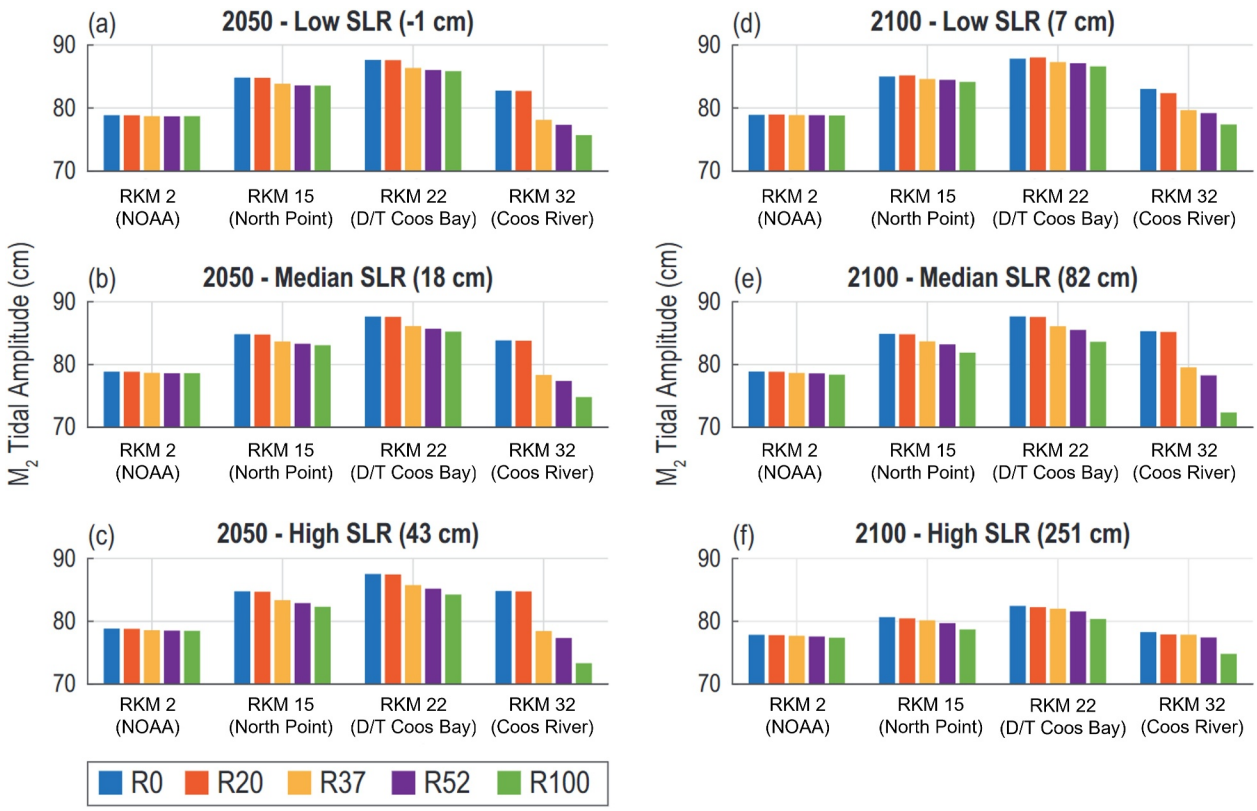


**Figure 7.** Modeled change to the $M_2$ tidal constituent amplitude for 2050 (left panels) and 2100 (right panels) under low (upper panels, a, d), median (middle panels, b, e), and high (lower panels, c, f) sea-level rise for five restoration scenarios (colored bars). Modeled phase changes resulting from wetland restoration for the same stations are shown via Figure S12 in Supporting Information S1.

2050 (Figure 8a). Under higher rates of SLR, the relationship becomes more non-linear, suggesting that a relatively greater increase in tidal prism resulting from wetland restoration is needed before there is a corresponding decrease in pWSE. Under the highest SLR scenario up to 2100, the increase in tidal prism with wetland restoration did not yield any reduction in pWSEs (Figure 8b).

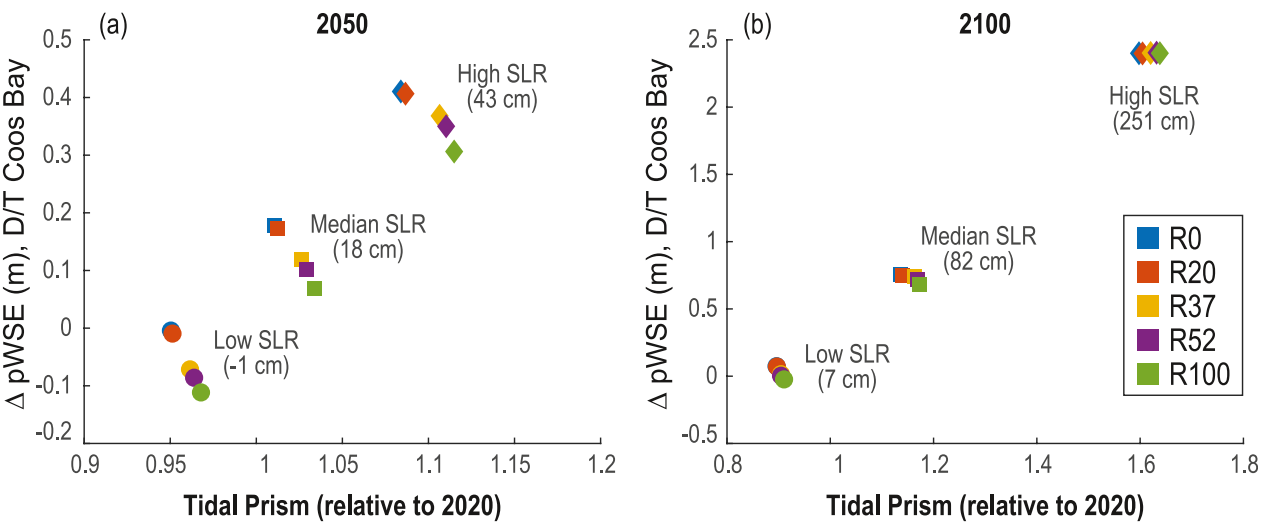


**Figure 8.** Projected changes in modeled peak water surface elevations (ΔpWSE, m) at downtown Coos Bay (RKM 22) and tidal prism for six sea-level rise and five restoration scenarios in Coos Bay for 2050 (a) and 2100 (b). Note that tidal prism calculations relative to present day (2020) for the R20 scenario (present day = 1).

## 5. Discussion

Nuisance flooding has been increasing in many parts of the world due to a combination of subsidence and SLR, with potentially significant economic and social impacts due to its disruptive nature. Wetland restoration has frequently been used to reduce the impacts of extreme storm events but has not yet been fully explored as a mechanism for reducing nuisance flooding. This paper couples a hydrodynamic with a harmonic model of water levels to implement a new method to quantify changes to nuisance flooding in an urban estuary as a result of both SLR and wetland restoration.

### 5.1. Threshold Effects of Wetland Restoration on Flooding Impacts

In this study, we project that tidal wetland restoration through levee removal in Coos Bay will reduce pWSEs and lessen the negative impacts of nuisance flooding in urban areas. However, we found that there may be important SLR thresholds that impact the effectiveness of wetland restoration for flood mitigation in the estuary over the 21st century. Wetland restoration appears to be most effective at reducing flood elevations at low to moderate levels of SLR (−1 to 43 cm), levels which are projected to occur by 2050 under lower emissions scenarios. This result stems from the additional accommodation space provided by floodplain wetland expansion to dampen the amplitude of the $M_2$ tidal constituent and reduce high water levels.

Greater rates of SLR (82–251 cm by 2100) limit the effectiveness of wetland restoration to reduce nuisance flooding. This is because the increased tidal volume resulting from substantially increased sea levels eventually exceeds the increased accommodation volume from restoration, reaching the limit of effectiveness in flood control capacity (i.e., Figure 8). Additionally, higher rates of SLR dampen estuarine $M_2$ amplitudes and upstream amplification through increases in the estuarine cross-sectional area due to levee overtopping, further limiting the ability of intertidal wetlands to modulate the tidal signal.

This study only investigated potential impacts due to tidal hydrodynamics (nuisance flooding); however, estuarine water levels in the PNW are also impacted by fluvial runoff and coastal storms that can cause significant changes in water levels, especially during compound extreme events (Helaire et al., 2020). Future work is needed to better quantify how wetland restoration could reduce flooding during and after these compound events, especially under different SLR and precipitation scenarios.

### 5.2. Physical Drivers of Reduced Nuisance Flooding

Tidal waves entering an estuary are distorted by friction, geometry, and intertidal storage in wetlands (Friedrichs et al., 1990). Friction and divergent geometry dampen the tidal range, while convergent geometry results in amplification. The interplay of friction and cross-sectional geometry can also induce ebb-flood asymmetries, which shift the durations of ebb and flood periods (Speer & Aubrey, 1985), which can affect nuisance flooding.

For this study, we considered two alterations to estuarine geometry that can impact nuisance flooding vulnerability in a PNW estuary: deepening by SLR and increased shallow water area through wetland restoration. In the absence of external factors such as levee overtopping, SLR will modify estuarine hydrodynamics by increasing water depth, which, like decreasing friction, tends to amplify tidal waves (Burchard, 2009; Ianniello, 1977). In contrast, wetlands tend to dampen flooding through increased friction, although this effect may be overwhelmed by channel deepening (Orton et al., 2015).

In our study, we anticipated decreases in tidal range due to amplitude reduction resulting from wetland restoration. This hypothesis was confirmed through the results: expanding wetland restoration in the estuary resulted in a reduction in the $M_2$ amplitude (e.g., from 87.5 to 83.6 cm in 2100 at RKM 22 under the median SLR scenario, Figure 7). Other constituents, such as $K_1$, also decreased in amplitude (from 47.0 to 45.5 cm for the same RKM and scenario, Figure S10 in Supporting Information S1).

Loss of tidal prism is a primary impact of land reclamation due to levee construction (Brew, 2010). Wetland restoration through levee removal reverses this effect, increasing tidal prism. The tidal prism increases due to SLR alone increases volumetric inflow by $6.7 \times 10^5$ $m^3$ under low SLR by 2050. The corresponding increase in estuarine volume due to restoration is $3.9 \times 10^7$ $m^3$, two orders of magnitude larger. This increase in estuarine volume due to restoration is responsible for the corresponding decreases in tidal amplitudes and nuisance flooding (Figure 8).

The reduction in tidal water level amplitudes due to wetland restoration may impact the capacity for wetlands to maintain pace with SLR due to changes to inundation dynamics. More work is needed to investigate the coupled impacts of tidal hydromodification through wetland restoration, especially changes to inundation and salinity regimes which could result in changes to plant communities.

Additionally, more studies are needed to investigate how changing estuarine friction affects tidal prism and corresponding flood risk in estuaries. For example, there could be tradeoffs between restoring different types of tidal wetlands. Historically, the Pacific Northwest contained extensive areas of Sitka spruce swamp (Brophy, 2019) which has a much higher hydraulic roughness compared to emergent marsh. Restoring swamps with higher hydraulic roughness in place of restoring emergent marshes may decrease overall wetland capacity to attenuate future flooding events in PNW estuaries but could have greater carbon sequestration or other benefits that outweigh the reduction in flood vulnerability. Furthermore, this study assumed that restoration involved full levee removal, while many wetland restoration activities involve partial removal (Hood, 2014). Further work could investigate how communities could optimize restoration design at the scales of individual sites and whole estuaries to meet multiple goals such as flood risk reduction, carbon sequestration, and fish habitat restoration.

### 5.3. Wetland Restoration as a Sea-Level Rise Adaptation Measure

In addition to many ecosystem-level benefits of tidal wetland restoration, this study demonstrates that natural infrastructure solutions can be an effective SLR adaptation measure for coastal communities by reducing nuisance flooding (or storm-associated flooding impacts) through tidal dampening. Without intervention, many of the agricultural areas now behind levees are expected to be regularly inundated in the future under moderate to higher SLR projections anyways, necessitating increases in levee heights, which will correspondingly increase tidal amplitudes (Jia, 2019; Wang et al., 2018).

Implementation of restoration as a SLR adaptation measure at the estuary scale could be planned in phases based on anticipated SLR impacts over the coming decades. For example, if models suggest 5 cm of SLR over the coming 1-2 decades, regional policy makers could choose to remove the levees at the two largest potential restoration projects and effectively retain the same risk of overtopping in downtown Coos Bay as today. This process could be repeated up to 10 cm of SLR, at which point further wetland restoration is not expected to result in a greater reduction in peak tidal elevations. While there are many other factors that go into local restoration planning, an adaptable approach can be responsive to landowner needs, flood vulnerability and community resources, and the need to enhance other ecosystem services. Coastal adaptation under rates of future SLR beyond 10 cm will likely require multiple strategies to avert flooding risk beyond wetland restoration, including gray infrastructure such as road and levee raising, and potentially managed retreat. Restoration funding mechanisms should incorporate the numerous ecosystem co-benefits associated with expanding wetlands including flooding, but also carbon sequestration and increased salmonoid habitat. New funding schemes such as Environmental Impact Bonds are well suited to capture these benefits and should be explored in future work (Brand et al., 2021).

Wetland restoration impacts on reducing estuarine nuisance flooding will depend on the ability of restored wetlands to keep pace with SLR through mineral sedimentation and organic matter production (Kirwan et al., 2013; Thorne et al., 2018). The Coos Bay watershed has an extensive history of logging, which has to date provided sufficient sediment supply for wetland accretion (Mathabane, 2015). It is possible that changes to upstream forest management or logging practices could decrease the availability of future sediment supplies, and thereby lower the historical accretion rates used for modeling in this study (Eidam et al., 2020). As demonstrated here and observed in other modeling studies (Brand et al., 2022; Kirwan et al., 2013; Thorne et al., 2018), wetland accretion will heavily depend on the global SLR pathway that occurs in the future. Both tidal flats and emergent marshes can accrete faster than current lower estimates of potential SLR. However, under moderate to high rates of SLR, our model suggests that Coos Bay wetlands will not be able to keep pace with rising sea levels, resulting in eventual marsh drowning and conversion to tidal flats/subtidal habitat, results consistent with model simulations for much of the west coast of the US (Thorne et al., 2018).

## 6. Conclusions

Our study developed a method for estimating future nuisance flooding in coastal estuaries using hydrodynamic modeling, accretion models, and tidal harmonic analysis. We show through a case study in southern Oregon that this approach can be used to assess the impacts of wetland restoration on future nuisance flooding. We found that

the flood reduction benefit associated with intertidal wetland restoration increased linearly up until the maximum feasible restoration under the low and median SLR scenarios. We also found that high SLR scenarios diminished or entirely eliminated the flood reduction benefits resulting from expanding restored wetlands in the estuary. As nuisance flooding becomes a greater concern in coastal areas throughout the world, scientists and planners will need different approaches to evaluate flooding risk and plan for adaptation.

Traditional flood protection measures such as raising roads and levees are typically designed with the sole purpose of protecting infrastructure, so those approaches may do little to enhance ecosystem co-benefits associated with tidal wetland restoration. In some cases, gray infrastructure projects may hinder wetland restoration opportunities by further isolating low elevation areas from estuarine connectivity. This study suggests that restoration can also be part of local and regional SLR adaptation strategies to reduce nuisance flooding. Coastal communities should evaluate these tradeoffs in their flood and SLR adaptation options before investing significant capital into flood protection infrastructure. Local decision-makers will need to work with private landowners in the PNW to plan and implement additional restoration measures since many restoration opportunities are on private land.

Coastal wetland restoration has many potential benefits beyond flood reduction. For instance, tidal wetlands in the PNW provide critical habitat for salmonids and migratory bird species, recreational opportunities that bolster tourism and resident access to green spaces, and water quality improvements through nutrient and sediment load absorption (Diefenderfer et al., 2016; Jackson et al., 2024; Thom et al., 2018). Tidal marshes and swamps also have substantial carbon storage and sequestration benefits regionally (Fitch et al., 2022; Kauffman et al., 2020; Peck et al., 2020). Future studies that investigate the flood reduction benefits of wetland restoration should also examine the costs and benefits of these additional ecosystem services and compare them with gray infrastructure options to mitigate estuarine flooding.

## Data Availability Statement

Water surface elevations used in both calibration and developing non-tidal residual elevations were taken from NOAA's Tides and Currents website (https://tidesandcurrents.noaa.gov/) for the Charleston, OR tide gauge (#9432780). Water depth calibration data for the remainder of the stations in Coos Bay are available from Conroy et al. (2020). Bathymetry was used from Conroy et al. (2020) and all sources listed therein. Marsh accretion data sets are open source and available from Brown et al. (2024): https://doi.org/10.25573/serc.25024448.v1. The Delft3D-FM model is open source and publicly available here: https://oss.deltares.nl/en/web/delft3dfm/home. The data on which this article is based are available in Brand et al. (2025).

**Acknowledgments**
This research was funded by the NOAA's Effects of Sea-level rise program (NA19NOS4780176) and NOAA's Direct Technical Assistance Grant (NA390B). The authors would also like to thank the Partnership for Coastal Watersheds (PCW) for their feedback on model design, outputs, and data throughout the project. We would also like to thank Bass Dye and Dave Sutherland for early contributions to the Coos Bay hydrodynamic model. We thank contributors to the Northeast Pacific Blue Carbon database, which helped facilitate regional calculations of wetland vertical accretion rates. Modeling was performed using PNNL Institutional Computing at Pacific Northwest National Laboratory. We gratefully acknowledge Tim Carlson of PNNL Institutional Computing for helping set up the Delft3D-FM model used in this study. Chris Mochon-Collura of US EPA assisted with core collection and processing. We thank the sea-level rise projection authors for developing and making the sea-level rise projections available, multiple funding agencies for supporting the development of the projections, and the NASA Sea-Level Change Team for developing and hosting the IPCC AR6 Sea-Level Projection Tool. The views expressed in this article are those of the authors and do not necessarily represent the views or policies of the U.S. Environmental Protection Agency. Any mention of trade names, products, or services does not imply an endorsement by the U.S. Government or the U.S. Environmental Protection Agency.

## References

Alizad, K., Hagen, S. C., Medeiros, S. C., Bilskie, M. V., Morris, J. T., Balthis, L., & Buckel, C. A. (2018). Dynamic responses and implications to coastal wetlands and the surrounding regions under sea level rise. *PLoS One*, *13*(10), e0205176. https://doi.org/10.1371/journal.pone.0205176

Alizad, K., Hagen, S. C., Morris, J. T., Bacopoulos, P., Bilskie, M. V., Weishampel, J. F., & Medeiros, S. C. (2016). A coupled, two-dimensional hydrodynamic-marsh model with biological feedback. *Ecological Modelling*, *327*, 29–43. https://doi.org/10.1016/j.ecolmodel.2016.01.013

Alizad, K., Morris, J. T., Bilskie, M. V., Passeri, D. L., & Hagen, S. C. (2022). Integrated modeling of dynamic marsh feedbacks and evolution under sea-level rise in a mesotidal estuary (Plum Island, MA, USA). *Water Resources Research*, *58*(8), e2022WR032225. https://doi.org/10.1029/2022wr032225

Barbier, E. B., Georgiou, I. Y., Enchelmeyer, B., & Reed, D. J. (2013). The value of wetlands in protecting southeast Louisiana from hurricane storm surges. *PLoS One*, *8*(3), e58715. https://doi.org/10.1371/journal.pone.0058715

Barth, N. A., Villarini, G., Nayak, M. A., & White, K. (2017). Mixed populations and annual flood frequency estimates in the western United States: The role of atmospheric rivers. *Water Resources Research*, *53*(1), 257–269. https://doi.org/10.1002/2016wr019064

Borde, A. B., Thom, R. M., Rumrill, S., & Miller, L. M. (2003). Geospatial habitat change analysis in Pacific Northwest coastal estuaries. *Estuaries*, *26*(4), 1104–1116. https://doi.org/10.1007/bf02803367

Brand, M. W., Buffington, K., Rogers, J. B., Thorne, K., Stein, E. D., & Sanders, B. F. (2022). Multi-decadal simulation of marsh topography under sea level rise and episodic sediment loads. *Journal of Geophysical Research: Earth's Surface*, *127*(9), e2021JF006526. https://doi.org/10.1029/2021JF006526

Brand, M. W., Diefenderfer, H. L., Cornu, C., McKeon, M., Janousek, C., Borde, A., et al. (2025). Dataset for: Can restoring tidal wetlands reduce nuisance flooding of coasts under future sea-level rise? [Dataset]. *DRYAD*. https://doi.org/10.5061/dryad.rv15dv4dw

Brand, M. W., Diefenderfer, H. L., O'Connor, J. E., Borde, A. B., Jay, D. A., Al-Bahadily, A., et al. (2023). Impacts of a Cascadia subduction zone earthquake on water levels and wetlands of the lower Columbia River and estuary. *Geophysical Research Letters*, *50*(14), e2023GL103017. https://doi.org/10.1029/2023gl103017

Brand, M. W., Seipp, K. Q., Saksa, P., Ulibarri, N., Bomblies, A., Mandle, L., et al. (2021). Environmental impact Bonds: A common framework and looking ahead. *Environmental Research: Infrastructure and Sustainability*, *1*(2), 023001. https://doi.org/10.1088/2634-4505/ac0b2c

Breithaupt, S., & Khangaonkar, T. (2008). Forensic hydrodynamic evaluation following the restoration of a tidal freshwater wetlands. In *Estuarine and coastal modeling (2007)* (pp. 618–632).

Brew, D. S., & Williams, P. B. (2010). Predicting the impact of large-scale tidal wetland restoration on morphodynamics and habitat evolution in south San Francisco Bay, California. *Journal of Coastal Research*, *26*(5), 912–924. https://doi.org/10.2112/08-1174.1

Brophy, L. S. (2019). *Comparing historical losses of forested, scrub-shrub, and emergent tidal wetlands on the Oregon coast, USA: A paradigm shift for estuary restoration and conservation*. Institute for Applied Ecology.

Brown, C. A., Mochon, C., Chris, T., & DeWitt, T. (2024). Dataset: Accretion rates and carbon sequestration in Oregon salt marshes [Dataset]. *Smithsonian Environmental Research Center*. https://doi.org/10.25573/serc.25024448.v1

Brunner, G. (2024). *HEC-RAS 2D user's manual*. US Army Corps of Engineers. Retrieved from https://www.hec.usace.army.mil/confluence/rasdocs/r2dum/latest

Burchard, H. (2009). Combined effects of wind, tide, and horizontal density gradients on stratification in estuaries and coastal seas. *Journal of Physical Oceanography*, *39*(9), 2117–2136. https://doi.org/10.1175/2009jpo4142.1

Burgos, A. G., Hamlington, B. D., Thompson, P. R., & Ray, R. D. (2018). Future nuisance flooding in Norfolk, VA, from astronomical tides and annual to decadal internal climate variability. *Geophysical Research Letters*, *45*(22), 412–432. https://doi.org/10.1029/2018gl079572

Conroy, T., Sutherland, D. A., & Ralston, D. K. (2020). Estuarine exchange flow variability in a seasonal, segmented estuary. *Journal of Physical Oceanography*, *50*(3), 595–613. https://doi.org/10.1175/JPO-D-19-0108.1

Diefenderfer, H. L., Borde, A. B., & Cullinan, V. I. (2021). Floodplain wetland channel planform, cross-sectional morphology, and sediment characteristics along an estuarine to tidal river gradient. *Journal of Geophysical Research: Earth Surface*, *126*(5), e2019JF005391. https://doi.org/10.1029/2019JF005391

Diefenderfer, H. L., Johnson, G. E., Thom, R. M., Buenau, K. E., Weitkamp, L. A., Woodley, C. M., et al. (2016). Evidence-based evaluation of the cumulative effects of ecosystem restoration. *Ecosphere*, *7*(3), e01242. https://doi.org/10.1002/ecs2.1242/epdf

Doodson, A. T. (1928). VI. The analysis of tidal observations. *Philosophical Transactions of the Royal Society of London - Series A: Containing Papers of a Mathematical or Physical Character*, *227*(647–658), 223–279.

Egbert, G. D., & Erofeeva, S. Y. (2002). Efficient inverse modeling of barotropic ocean tides. *Journal of Atmospheric and Oceanic Technology*, *19*(2), 183–204. https://doi.org/10.1175/1520-0426(2002)019<0183:eimobo>2.0.co;2

Eidam, E. F., Souza, T., Keogh, M., Sutherland, D., Schmitt, J., & Helms, A. (2023). Sediment grain size, organic content, and Pb-210 excess activity in Coos Bay from 2021-05-17 to 2021-05-19 (NCEI Accession 0277842) [Dataset]. *NOAA National Centers for Environmental Information*. https://doi.org/10.25921/ywjy-3f15

Eidam, E. F., Sutherland, D. A., Ralston, D. K., Dye, B., Conroy, T., Schmitt, J., et al. (2020). Impacts of 150 years of shoreline and bathymetric change in the Coos Estuary, Oregon, USA. *Estuaries and Coasts*, *45*(4), 1–19. https://doi.org/10.1007/s12237-020-00732-1

Fant, C., Jacobs, J. M., Chinowsky, P., Sweet, W., Weiss, N., Sias, J. E., et al. (2021). Mere nuisance or growing threat? The physical and economic impact of high tide flooding on US road networks. *Journal of Infrastructure Systems*, *27*(4), 04021044. https://doi.org/10.1061/(asce)is.1943-555x.0000652

Fitch, A. A., Blount, K., Reynolds, L., & Bridgham, S. D. (2022). Partial recovery of microbial function in restored coastal marshes of Oregon, USA. *Soil Science Society of America Journal*, *86*(3), 831–846. https://doi.org/10.1002/saj2.20383

Flick, R. E. (2000). Time-of-day of peak tides in a mixed-tide regime. *Shore and Beach*, *68*(4), 15–17.

Fox-Kemper, B., Hewitt, H. T., Xiao, C., Aðalgeirsdóttir, G., Drijfhout, S. S., Edwards, T. L., et al. (2021). Ocean, cryosphere and sea level change. In V. Masson-Delmotte, P. Zhai, A. Pirani, S. L. Connors, C. Péan, S. Berger, et al. (Eds.), *Climate change 2021: The physical science basis. Contribution of working group I to the sixth assessment report of the intergovernmental panel on climate change* (pp. 1211–1362). Cambridge University Press. https://doi.org/10.1017/9781009157896.011

Friedrichs, C. T., Aubrey, D. G., & Speer, P. E. (1990). Impacts of relative Sea-level rise on evolution of shallow estuaries. In R. T. Cheng (Ed.), *Residual currents and long-term transport. Coastal and estuarine studies* (Vol. 38, pp. 105–122). Springer. https://doi.org/10.1007/978-1-4613-9061-9_9

Garner, G. G., Hermans, T., Kopp, R. E., Slangen, A. B. A., Edwards, T. L., Levermann, A., et al. (2021). IPCC AR6 sea-level rise projections. Version 20210809. https://sealevel.nasa.gov/ipcc-ar6-sea-level-projection-tool/?psmsl_id=1269&data_layer=scenario

Gourevitch, J. D., Diehl, R. M., Wemple, B. C., & Ricketts, T. H. (2022). Inequities in the distribution of flood risk under floodplain restoration and climate change scenarios. *People and Nature*, *4*(2), 415–427. https://doi.org/10.1002/pan3.10290

Haddad, J., Lawler, S., & Ferreira, C. M. (2016). Assessing the relevance of wetlands for storm surge protection: A coupled hydrodynamic and geospatial framework. *Natural Hazards*, *80*(2), 839–861. https://doi.org/10.1007/s11069-015-2000-7

Helaire, L. T., Talke, S. A., Jay, D. A., & Chang, H. (2020). Present and future flood hazard in the lower Columbia river estuary: Changing flood hazards in the Portland-Vancouver metropolitan area. *Journal of Geophysical Research: Oceans*, *125*(7), e2019JC015928. https://doi.org/10.1029/2019jc015928

Hino, M., Belanger, S. T., Field, C. B., Davies, A. R., & Mach, K. J. (2019). High-tide flooding disrupts local economic activity. *Science Advances*, *5*(2), eaau2736. https://doi.org/10.1126/sciadv.aau2736

Hoitink, A. J. F., & Jay, D. A. (2016). Tidal river dynamics: Implications for deltas. *Reviews of Geophysics*, *54*(1), 240–272. https://doi.org/10.1002/2015rg000507

Holleman, R. C., & Stacey, M. T. (2014). Coupling of sea level rise, tidal amplification, and inundation. *Journal of Physical Oceanography*, *44*(5), 1439–1455. https://doi.org/10.1175/jpo-d-13-0214.1

Hood, W. G. (2014). Differences in tidal channel network geometry between reference marshes and marshes restored by historical dike breaching. *Ecological Engineering*, *71*, 563–573. https://doi.org/10.1016/j.ecoleng.2014.07.076

Ianniello, J. (1977). Tidally induced residual currents in estuaries of constant breadth and depth. *Journal of Marine Research*, *35*, 755–786.

IPCC. (2014). *Climate change 2014: Synthesis report. Contribution of working groups I, II and III to the fifth assessment report of the intergovernmental panel on climate change*. In R. K. Pachauri & L. A. Meyer (Eds.), (p. 151).

Jackson, C. A., Hernandez, C. L., Yee, S. H., Nash, M. S., Diefenderfer, H. L., Borde, A. B., et al. (2024). Identifying priority ecosystem services in tidal wetland restoration. *Frontiers in Ecology and Evolution*, *12*. https://doi.org/10.3389/fevo.2024.1260447

Jacobs, J. M., Cattaneo, L. R., Sweet, W., & Mansfield, T. (2018). Recent and future outlooks for nuisance flooding impacts on roadways on the US East Coast. *Transportation Research Record*, *2672*(2), 1–10. https://doi.org/10.1177/0361198118756366

Jia, G., Wang, R. Q., & Stacey, M. T. (2019). Investigation of impact of shoreline alteration on coastal hydrodynamics using Dimension Reduced Surrogate based Sensitivity Analysis. *Advances in Water Resources*, *126*, 168–175. https://doi.org/10.1016/j.advwatres.2019.03.001

Karegar, M. A., Dixon, T. H., Malservisi, R., Kusche, J., & Engelhart, S. E. (2017). Nuisance flooding and relative sea-level rise: The importance of present-day land motion. *Scientific Reports*, *7*, 1–9. https://doi.org/10.1038/s41598-017-11544-y

Kauffman, J. B., Giovanonni, L., Kelly, J., Dunstan, N., Borde, A., Diefenderfer, H., et al. (2020). Total ecosystem carbon stocks at the marine-terrestrial interface: Blue carbon of the Pacific Northwest Coast, United States. *Global Change Biology*, *26*(10), 5679–5692. https://doi.org/10.1111/gcb.15248

Kernkamp, H. W., Van Dam, A., Stelling, G. S., & de Goede, E. D. (2011). Efficient scheme for the shallow water equations on unstructured grids with application to the Continental Shelf. *Ocean Dynamics*, *61*(8), 1175–1188. https://doi.org/10.1007/s10236-011-0423-6

Kirwan, M. L., & Megonigal, J. P. (2013). Tidal wetland stability in the face of human impacts and sea-level rise. *Nature*, *504*(7478), 53–60. https://doi.org/10.1038/nature12856

Kirwan, M. L., Temmerman, S., Skeehan, E. E., Guntenspergen, G. R., & Fagherazzi, S. (2016). Overestimation of marsh vulnerability to sea level rise. *Nature Climate Change*, *6*(3), 253–260. https://doi.org/10.1038/nclimate2909

Kopp, R. E., DeConto, R. M., Bader, D. A., Hay, C. C., Horton, R. M., Kulp, S., et al. (2017). Evolving understanding of Antarctic ice-sheet physics and ambiguity in probabilistic sea-level projections. *Earth's Future*, *5*(12), 1217–1233. https://doi.org/10.1002/2017ef000663

Kopp, R. E., Garner, G. G., Hermans, T. H., Jha, S., Kumar, P., Slangen, A. B., et al. (2023). The framework for assessing changes to Sea-level (FACTS) v1. 0-rc: A platform for characterizing parametric and structural uncertainty in future global, relative, and extreme sea-level change. *EGUsphere*, *2023*, 1–34.

Kopp, R. E., Oppenheimer, M., O'Reilly, J. L., Drijfhout, S. S., Edwards, T. L., Fox-Kemper, B., et al. (2023). Communicating future sea-level rise uncertainty and ambiguity to assessment users. *Nature Climate Change*, *13*(7), 648–660. https://doi.org/10.1038/s41558-023-01691-8

Lee, H., & Brown, C. A. (2009). Classification of regional patterns of environmental drivers and benthic habitats in Pacific Northwest estuaries. In *U.S. EPA, office of research and development, national health and environmental effects research laboratory, western ecology division*. EPA/600/R-09/140.

Lesser, G. R., Roelvink, J. V., van Kester, J. T. M., & Stelling, G. S. (2004). Development and validation of a three-dimensional morphological model. *Coastal engineering*, *51*(8–9), 883–915. https://doi.org/10.1016/j.coastaleng.2004.07.014

Loder, N. M., Irish, J. L., Cialone, M. A., & Wamsley, T. V. (2009). Sensitivity of hurricane surge to morphological parameters of coastal wetlands. *Estuarine, Coastal and Shelf Science*, *84*(4), 625–636. https://doi.org/10.1016/j.ecss.2009.07.036

Lu, C., Zhang, F., Jia, J., & Wang, Y. P. (2024). Impact of sea level rise on tidal energy budget in a macro-tidal coastal bay with archipelago. *Frontiers in Marine Science*, *10*. https://doi.org/10.3389/fmars.2023.1302800

Mathabane, N. (2015). *Potential impacts of timber harvesting, climate, and conservation on sediment accumulation and dispersal in the South Slough National Estuarine Reserve, Oregon* (Doctoral dissertation). University of Oregon.

Moftakhari, H. R., AghaKouchak, A., Sanders, B. F., Allaire, M., & Matthew, R. A. (2018). What is nuisance flooding? Defining and monitoring an emerging challenge. *Water Resources Research*, *54*(7), 4218–4227. https://doi.org/10.1029/2018wr022828

Moftakhari, H. R., AghaKouchak, A., Sanders, B. F., Feldman, D. L., Sweet, W., Matthew, R. A., & Luke, A. (2015). Increased nuisance flooding along the coasts of the United States due to sea level rise: Past and future. *Geophysical Research Letters*, *42*(22), 9846–9852. https://doi.org/10.1002/2015gl066072

Moftakhari, H. R., AghaKouchak, A., Sanders, B. F., & Matthew, R. A. (2017). Cumulative hazard: The case of nuisance flooding. *Earth's Future*, *5*(2), 214–223. https://doi.org/10.1002/2016ef000494

Morris, J. T., Sundareshwar, P. V., Nietch, C. T., Kjerfve, B., & Cahoon, D. R. (2002). Responses of coastal wetlands to rising sea level. *Ecology*, *83*(10), 2869–2877. https://doi.org/10.2307/3072022

NOAA. (2023). Sea level trends - NOAA tides & currents. Retrieved from https://tidesandcurrents.noaa.gov/sltrends/sltrends_station.shtml?id=9432780

O'Brien, F. E. (2017). Statewide levee database for Oregon, release 1.0: Major agricultural and urban areas in western Oregon and along the Columbia river. DOGAMI open file report: O-17-02. Retrieved from https://www.oregongeology.org/pubs/ofr/p-O-17-02.htm

OCM Partners. (2023). 2014 USACE NWP topobathy lidar: Coos bay (OR). Retrieved from https://www.fisheries.noaa.gov/inport/item/49941

Orton, P. M., Talke, S. A., Jay, D. A., Yin, L., Blumberg, A. F., Georgas, N., et al. (2015). Channel shallowing as mitigation of coastal flooding. *Journal of Marine Science and Engineering*, *3*(3), 654–673. https://doi.org/10.3390/jmse3030654

Pawlowicz, R., Beardsley, B., & Lentz, S. (2002). Classical tidal harmonic analysis including error estimates in MATLAB using T_TIDE. *Computers & Geosciences*, *28*(8), 929–937. https://doi.org/10.1016/s0098-3004(02)00013-4

Peck, E. K., Wheatcroft, R. A., & Brophy, L. S. (2020). Controls on sediment accretion and blue carbon burial in tidal saline wetlands: Insights from the Oregon coast, USA. *Journal of Geophysical Research: Biogeosciences*, *125*(2), e2019JG005464. https://doi.org/10.1029/2019jg005464

Ray, R. D., & Foster, G. (2016). Future nuisance flooding at Boston caused by astronomical tides alone. *Earth's Future*, *4*(12), 578–587. https://doi.org/10.1002/2016EF000423

Rumrill, S. S. (2006). The ecology of the south slough estuary: Site profile of the south slough national estuarine research Reserve. *Charleston, OR: South Slough National Estuarine Research Reserve*, 238.

Schile, L. M., Callaway, J. C., Morris, J. T., Stralberg, D., Parker, V. T., & Kelly, M. (2014). Modeling tidal marsh distribution with sea-level rise: Evaluating the role of vegetation, sediment, and upland habitat in marsh resiliency. *PLoS One*, *9*(2), e88760. https://doi.org/10.1371/journal.pone.0088760

Shennan, I. A. N., Milne, G., & Bradley, S. (2012). Late holocene vertical land motion and relative sea-level changes: Lessons from the British isles. *Journal of Quaternary Science*, *27*(1), 64–70. https://doi.org/10.1002/jqs.1532

Shepard, C. C., Crain, C. M., & Beck, M. W. (2011). The protective role of coastal marshes: A systematic review and meta-analysis. *PLoS One*, *6*(11), e27374. https://doi.org/10.1371/journal.pone.0027374

Smolders, S., Plancke, Y., Ides, S., Meire, P., & Temmerman, S. (2015). Role of intertidal wetlands for tidal and storm tide attenuation along a confined estuary: A model study. *Natural Hazards and Earth System Sciences*, *15*(7), 1659–1675. https://doi.org/10.5194/nhess-15-1659-2015

Speer, R. E., & Aubrey, D. G. (1985). A Study of non-linear tidal propagation in shallow inlet/estuarine systems, Part II Theory. *Estuarine, Coastal and Shelf Science*, *21*(2), 207–224. https://doi.org/10.1016/0272-7714(85)90097-6

Sweet, W. V., Hamlington, B. D., Kopp, R. E., Weaver, C. P., Barnard, P. L., Bekaert, D., et al. (2022). *Global and regional sea level rise scenarios for the United States: Updated mean projections and extreme water level probabilities along U.S. Coastlines*. NOAA Technical Report NOS 01. National Oceanic and Atmospheric Administration, National Ocean Service. https://oceanservice.noaa.gov/hazards/sealevelrise/noaa-nostechrpt01-global-regional-SLR-scenarios-US.pdf

Sweet, W. V., Kopp, R. E., Weaver, C. P., Obeysekera, J., Horton, R. M., Thieler, E. R., & Zervas, C. (2017). *Global and regional sea level rise scenarios for the United States*. National Oceanic and Atmospheric Administration. (No. CO-OPS 083).

Sweet, W. V., & Park, J. (2014). From the extreme to the mean: Acceleration and tipping points of coastal inundation from sea level rise. *Earth's Future*, *2*(12), 579–600. https://doi.org/10.1002/2014EF000272

Thom, R. M., Breithaupt, S. A., Diefenderfer, H. L., Borde, A. B., Roegner, G. C., Johnson, G. E., & Woodruff, D. L. (2018). Storm-driven particulate organic matter flux connects a tidal tributary floodplain wetland, mainstem river, and estuary. *Ecological Applications*, *28*(6), 1420–1434. https://doi.org/10.1002/eap.1759

Thorne, K., MacDonald, G., Guntenspergen, G., Ambrose, R., Buffington, K., Dugger, B., et al. (2018). US Pacific coastal wetland resilience and vulnerability to sea-level rise. *Science Advances*, *4*(2), eaao3270. https://doi.org/10.1126/sciadv.aao3270

Thorne, K. M., Dugger, B. D., Buffington, K. J., Freeman, C. M., Janousek, C. N., Powelson, K. W., et al. (2015). Marshes to mudflats – Effects of sea-level rise on tidal marshes along a latitudinal gradient in the Pacific Northwest. *U.S. Geological Survey Open-File Report 2015-1204*, 54.

United States Census Bureau. (2022). 2020 Census results. Retrieved from https://www.census.gov/on6/10/2023

US Geological Survey. (2019). National land cover database. Retrieved from https://www.usgs.gov/centers/eros/science/national-land-cover-database?qt-science_center_objects=0#qt-science_center_objects

Wamsley, T. V., Cialone, M. A., Smith, J. M., Atkinson, J. H., & Rosati, J. D. (2010). The potential of wetlands in reducing storm surge. *Ocean Engineering*, *37*(1), 59–68. https://doi.org/10.1016/j.oceaneng.2009.07.018

Wang, R. Q., Stacey, M. R., Herdman, L. M. M., Barnard, P. L., & Erikson, L. (2018). The influence of sea level rise on the regional interdependence of coastal infrastructure. *Earth's Future*, *6*(5), 677–688. https://doi.org/10.1002/2017ef000742